Journal of The Electrochemical Society, **149** (2) A127-A132 (2002)
0013-4651/2001/149(2)/A127/6/$7.00 © The Electrochemical Society, Inc.

Effect of Al_2O_3-Coated *o*-$LiMnO_2$ Cathodes Prepared at Various Temperatures on the 55°C Cycling Behavior

Jaephil Cho,[a,*,z] Yong Jeong Kim,[b,] Tae-Joon Kim,[b,**] and Byungwoo Park[b,*]**

[a]*Samsung SDI Company Limited, Energy Laboratory, Research and Development Center, Chonan, Chungchongnam-Do, Korea*
[b]*School of Materials Science and Engineering, Seoul National University, Seoul, Korea*

The electrochemical cycling behavior of Al_2O_3-coated orthorhombic $LiMnO_2$ (*o*-$LiMnO_2$) cathodes prepared at various temperatures (150-700°C) is reported. While the coated *o*-$LiMnO_2$ cathodes prepared at 600 and 700°C show that Al atoms are uniformly distributed throughout the particle, those prepared at 400 and 500°C show that Al atoms are mainly located at the surface region. This difference significantly affects both the discharge capacity and the cycle life of the electrodes, and lower temperature heat-treatment of the coated *o*-$LiMnO_2$ results in a higher capacity and a better cycle life during 55°C cycling. In particular, coated cathodes prepared at 400°C exhibit the best cycling performance, maintaining a maximum capacity of bare *o*-$LiMnO_2$, with a minimal capacity loss. Moreover, capacity fading is closely related to Mn dissolution from $LiMn_2O_4$ and $Li_2Mn_2O_4$ phases appeared over the 3 and 4 V cycling, respectively.
 [DOI: 10.1149/1.1429927]

Manuscript submitted December 4, 2000; revised manuscript received September 18, 2001. Available electronically December 20, 2001.

Orthorhombic $LiMnO_2$ (*o*-$LiMnO_2$) is an interesting intercalation compound used as a cathode for lithium batteries due to its high theoretical capacity (285 mAh/g). This cathode material has been known since 1956, and has a space group of *Pmnm*.[1] It has been reported that *o*-$LiMnO_2$ transforms to a phase having spinel-like ordering during cycling, which has been confirmed by both X-ray diffraction (XRD) of the cycled electrodes and the appearance of the 4 and 3 V plateaus in the charge/discharge curves.[2-4] Well-ordered *o*-$LiMnO_2$ prepared above 800°C shows no significant capacity fading at room-temperature cycling over both the 4 and 3 V plateaus, unlike *o*-$LiMnO_2$ prepared at low temperatures (<500°C).[5] Even though poor cyclability over the 3 V plateau in $Li_xMn_2O_4$ has been attributed to the mechanical failure resulting from the 16% increase in the c/a ratio, induced by the collective Jahn-Teller distortion,[6-8] cyclability was significantly improved in *o*-$LiMnO_2$ by the creation of nanodomains of 5-20 nm upon transformation to cubic spinel.[9] However, an *o*-$LiMnO_2$ cathode showed more rapid capacity fading at 55°C compared to the room temperature cycling, exhibiting a 20% capacity loss of its maximum capacity of 180 mAh/g at charge and discharge currents of 150 and 75 mA/g, respectively, between 4.4 and 2.5 V after 100 cycles.[4]

Mn dissolution in $LiMn_2O_4$ spinel was the origin of elevated-temperature poor cycling performance, leading to the formation of defect-type spinels.[10-14] The Mn dissolution was induced by acids generated from reactions of $LiPF_6$ salts with the water impurities present in the cell components.[15,16] This reaction results in the formation of HF, which drastically increases the dissolution of Mn cations through a disproportionation reaction of Mn^{3+}

$$2Mn^{3+} \rightarrow Mn^{2+} + Mn^{4+} \quad [1]$$

Robertson *et al.* suggested that the capacity decay is attributed to the disproportionation of the spinel electrode into an acid-soluble species (Mn^{2+}), and compounds containing Mn^{4+} ions, such as $Li_2Mn_4O_9$ and Li_2MnO_3.[12]

In the study of Li-Mn-O spinel electrodes that were stored at 55°C in a 1 M $LiPF_6$, ethylene carbonate (EC)/dimethyl carbonate (DMC) electrolyte, Blyr *et al.* reported that manganese dissolution changes the spinel composition with a concomitant formation of rock salt Li_2MnO_3.[13] The capacity fading that occurs in $Li_xMn_2O_4$ is also associated with structural degradation of the spinel electrode and the formation of Li_2MnO_3 at the particle surface. The presence of Li_2MnO_3 is attributed to MnO dissolution from $Li_2Mn_2O_4$, which is generated as an over-discharged product on the surface of $LiMn_2O_4$ spinel electrode.[17]

In order to improve the structural stability of the *o*-$LiMnO_2$ cathode during 55°C cycling, a partial substitution of Mn with Al in $Li_xMn_{1-y}Al_yO_2$ was studied by Chiang *et al.*[4] However, this cation substitution reduces the initial capacity by 30 mAh/g and maximum capacity to 150 mAh/g. An alternative approach improving the structural stability is by coating the *o*-$LiMnO_2$ surface with metal oxides such that a higher concentration of metal atoms at the surface may minimize the structural instability from HF attack. Sol-gel coating of $LiCoO_2$ on $LiMn_2O_4$ particles with subsequent heat-treatments at 800°C has been demonstrated to be very effective for improving the structural stability of $LiMn_2O_4$ at 55°C cycling.[18] With a similar strategy, sol-gel coating of different metal oxides with subsequent heat-treatment may solve the serious capacity fading problem during electrochemical cycling in $LiCoO_2$ cathode materials.[19]

In this article, we report the effect of electrochemical cycling on *o*-$LiMnO_2$ cathode materials that were prepared with a sol-gel coating of Al_2O_3, and subsequent heat-treatments at various temperatures ranging from 150 to 700°C. This sol-gel coating provides a means of controlling the specific capacity depending on the heat-treatment conditions.

Experimental

o-$LiMnO_2$ powders were prepared using stoichiometric amounts of $LiOH{\cdot}H_2O$ and Mn_2O_3 (1.05:1 mol ratio) and heating at 800°C for 24 h under N_2 or Ar atmospheres. An excess amount of Li (0.05 mol) was used to compensate for the loss of Li during firing. To coat Al_2O_3 on the *o*-$LiMnO_2$ powder surface (with an average particle size of 13 μm), aluminum ethylhexanodiisopropoxide $Al(OOC_8H_{15})(OC_3H_7)_2$ was first dissolved in 2-propanol, followed by continuous stirring for 20 h at 21°C. The powders were then mixed with the coating solution such that the total amount of the coating solution corresponded to 15 wt % of the *o*-$LiMnO_2$ powders used. Metal alkoxides of $Al(OR)_4$ were first hydrolyzed into $Al(OR)_3(OH)$ by a reaction with H_2O in the atmosphere. Subsequently, the Al-OH groups in the hydrolyzed alkoxides $Al(OR)_3(OH)$ were polycondensed into Al-OR groups to form $(OR)_3Al\text{-}O\text{-}Al(OR)_3$ within the coating layer. Finally, the Al-OR

* Electrochemical Society Active Member.
** Electrochemical Society Student Member.
z E-mail: jpcho@samsung.co.kr

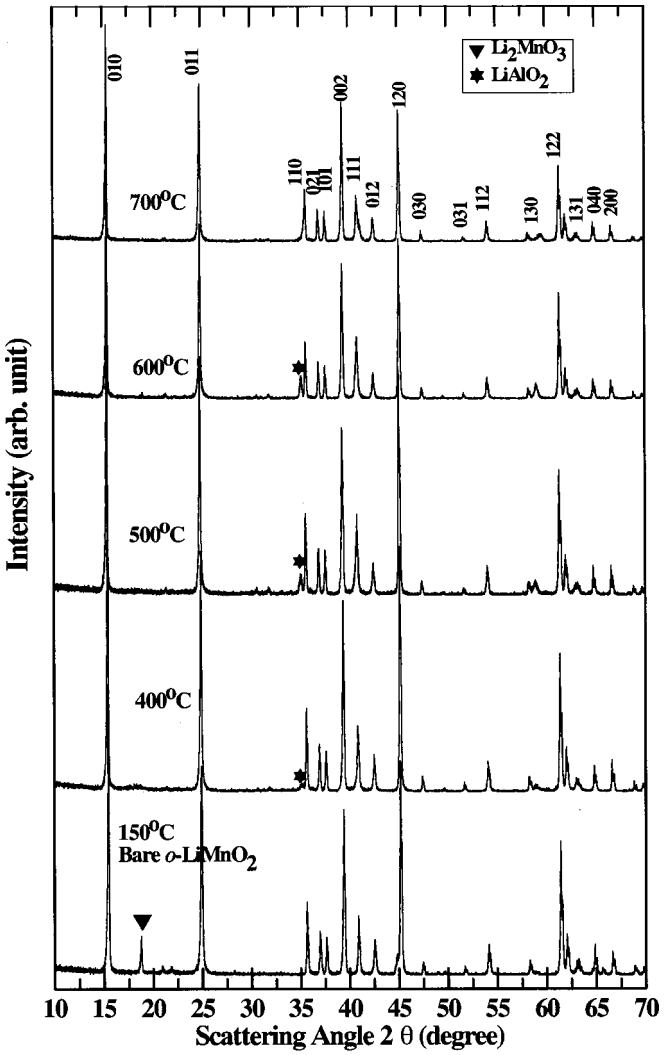

Figure 1. XRD patterns of coated *o*-$LiMnO_2$ powders prepared by sol-gel coating of Al_2O_3 at 150, 400, 500, 600, and 700°C.

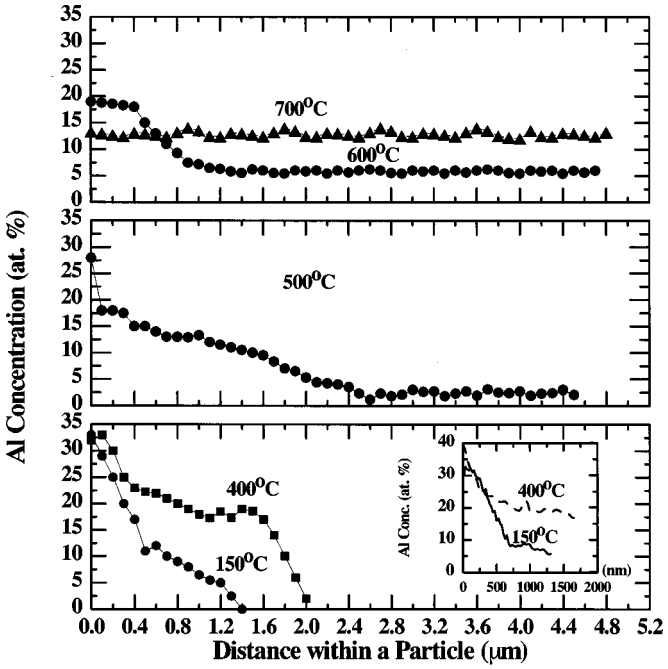

Figure 2. EPMA analysis of the Al atoms in the coated *o*-$LiMnO_2$ prepared at 150, 400, 500, 600, and 700°C as a function of distance within a particle. Inset: AES depth profile of Al atoms in coated *o*-$LiMnO_2$ prepared at 150 and 400°C.

groups reacted with the *o*-$LiMnO_2$ surface-OH groups, resulting in a good adhesion of the Al_2O_3 gel to the *o*-$LiMnO_2$ particle surface. During firing, the Al alkoxide gel on the *o*-$LiMnO_2$ surface-O-$Al(OR)_3$ was first decomposed into amorphous Al_2O_3 and then crystallized. After drying the *o*-$LiMnO_2$ powders coated with the aluminum alkoxide gel at 150°C for 10 h, the batches were then fired at 400, 500, 600, and 700°C, respectively, for 10 h in a dried air atmosphere.

For electrochemical testing, cathode slurry was prepared by mixing the oxide powders, carbon black (Super P), and poly(vinylidene) fluoride (PVDF) in the weight ratio of 92:4:4. When the slurry reached an appropriate viscosity, it was coated on an aluminum foil using a minicoater, and the *n*-methylpyrrolidone was completely evaporated at 150°C for 1 h in an oven. The cathode plate was then pressed into an appropriate thickness in a roll press, and blanked into a disk 1 cm in diam with 25 mg of active material. The samples were then vacuum dried at 140°C for 1 h, and transferred to an argon-filled glove box. Coin-type cells (2016 size) contained *o*-$LiMnO_2$ powders, a polyethylene microfilm separator, and Li metal. The electrolyte was 1.3 M $LiPF_6$ dissolved in a mixture of EC/DMC/ethylmethyl carbonate (EC/DMC/EMC) (3/3/4 vol %). To ensure that the capacity fading of the coin cell was not due to the Li-metal anode, some coin cells were disassembled after 50 cycles, and the cell was remade replacing the cycled Li-metal anode with fresh Li. These remade cells showed similar capacity within 170 mAh/g, comparable to those of the matching original cells after 50 cycles. This confirmed that the capacity fading of the original cell after cycling was due to the cathode. XRD patterns were taken after 50 cycles using the electrodes that were prepared as follows: the cycling tests were stopped at the end of discharge at 2 V and held at this voltage for 20 h. The cells were then dissembled carefully in a glove box to remove the cathode. The sample cathode was subsequently washed with DMC to remove the $LiPF_6$, followed by drying in a vacuum oven at 80°C for 24 h. An electron probe microanalysis (EPMA, JXA-8900R, JEOL) was used to measure the Al concentration profile from a cross-sectioned particle, and Auger electron spectroscopy (AES) with sputtering was used for the concentration profile in the vicinity of the particle surface.

Results and Discussion

The XRD patterns of the Al_2O_3-coated *o*-$LiMnO_2$ samples prepared at 150, 400, 500, 600, and 700°C are shown in Fig. 1. A small concentration of Li_2MnO_3 phase was observed in the coated $LiMnO_2$ specimen prepared at 150°C, which is similar to the case of bare *o*-$LiMnO_2$, but it disappeared at 400°C. The formation of the Li_2MnO_3 phase was due to a reaction with oxygen in the atmosphere. Since this phase disappeared after heat-treatment at 400°C, Li_2MnO_3 was probably distributed mainly at the surface, thus decomposing to $LiAlO_2$ and $LiMnO_2$ (Fig. 1). However, the $LiAlO_2$ phase disappeared after heat-treatment at 700°C (Fig. 1). In addition, the splitting of (130) diffraction peak is interesting, increasing with heat-treatment temperature. A full-width-at-half-maximum (FWHM) of the (011) peak from bare and 400°C samples, which is indicative of the degree of stacking faults between the Mn and Li sites, was approximately $\Delta(2\theta) = 0.096°$ (after correcting with the instrumental resolution function), corresponding to <1% stacking faults.[20] However, this width is wider than that of *o*-$LiMnO_2$ (0.015°) reported by Jang *et al.*[5] indicating the formation of a more disordered orthorhombic structure.

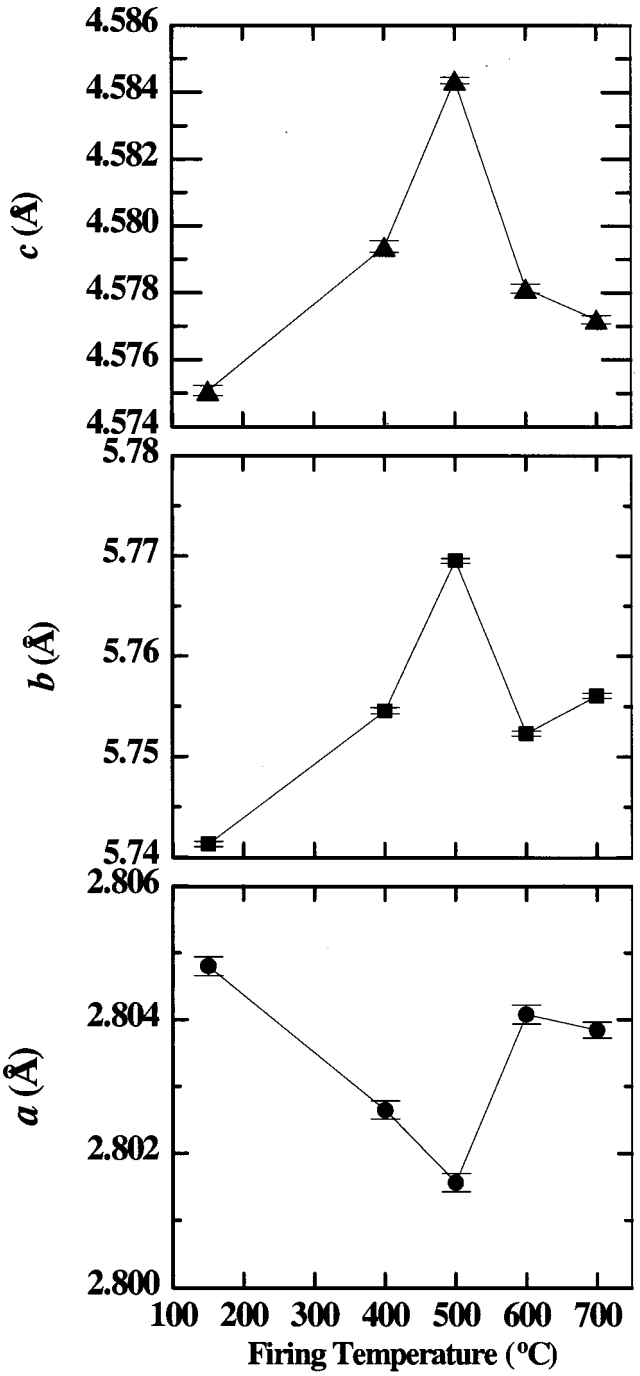

Figure 3. Plots of the lattice constants *a*, *b*, and *c* as a function of heat-treatment temperature.

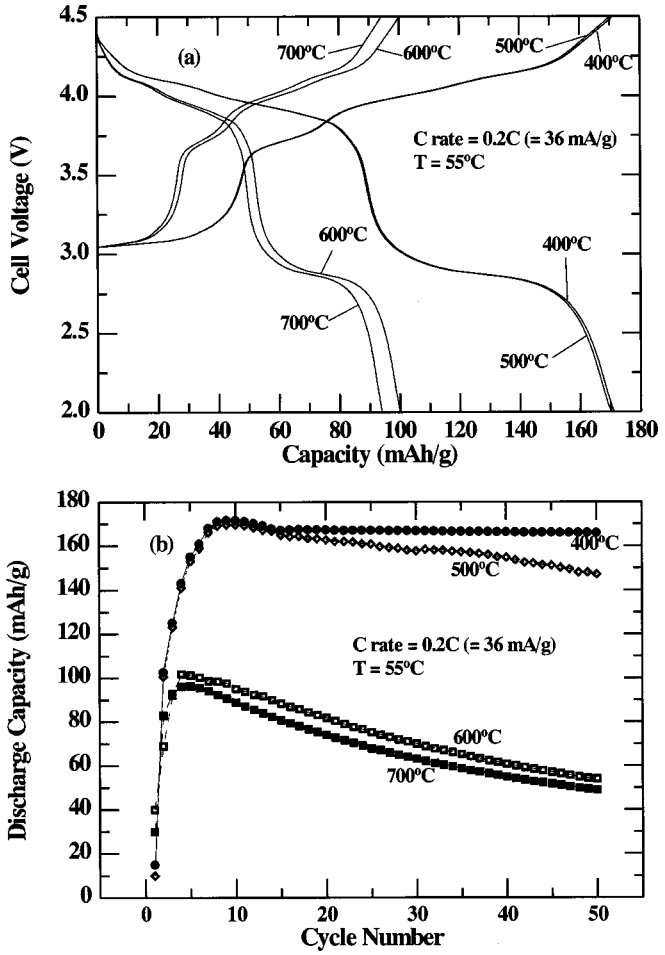

Figure 4. Plots of (a) cell voltage *vs.* capacity in coated $LiMnO_2$ prepared at 400, 500, 600, and 700°C after six cycles, and (b) discharge capacity *vs.* cycle number in coated $LiMnO_2$ prepared at 400, 500, 600, and 700°C.

Although the XRD patterns do not show evidence of Al_2O_3 or $LiMn_{1-x}Al_xO_2$ formation from a reaction between the Al_2O_3 gel and *o*-$LiMnO_2$, $LiAlO_2$ formation as a minor peak indicates that the Al_2O_3 gel solution reacted with the *o*-$LiMnO_2$ at the surface. In order to further investigate the distribution of Al atoms throughout the particle after coating, EPMA was used to map its distribution, as shown in Fig. 2. Coated samples prepared at 150, 400, and 500°C show that Al atoms are distributed within the ~1μm region. However, heat-treatments at higher temperatures (600 and 700°C) lead a deeper diffusion of Al atoms into the particle. This is consistent with AES of samples prepared at 150 and 400°C, showing the formation of a $LiMn_{1-x}Al_xO_2$ solid solution in the vicinity of the surface (an inset in Fig. 2). A sputtering rate of 260 Å/min obtained from standard SiO_2 is assumed to have the same sputtering rate in the present sample.

The different distribution of Al atoms in the surface region clearly affects lattice constants of the orthorhombic phase, *a*, *b*, and *c*. The lattice constant *a* decreases up to 500°C, while *b* and *c* increase up to 500°C (Fig. 3). However, the lattice constants, *b* and *c*, decrease at 600 and 700°C. The increasing lattice constants, *b* and *c*, up to 500°C is probably due to the discretely higher Al concentration at the surface than in the bulk. However, the trend at 600 and 700°C is believed to be due to deeper diffusion of Al atoms into the particle. A similar behavior was also observed in SnO_2-coated $LiCoO_2$.[18]

Such a different Al distribution also influences the cycling behavior of coated electrodes, showing large capacity variation depending on the heat-treatment temperature. The discharge capacities of the coated electrodes prepared at 400 and 500°C are 170 and 167 mAh/g, respectively, between 4.5 and 2 V at a rate of 0.2 C (36 mA/g) after six cycles. However, those prepared at 600 and 700°C show a rapid decrease to 100 and 95 mAh/g, respectively (Fig. 4a). Note that capacities of the coated samples prepared at 400 and 500°C are similar to that of bare *o*-$LiMnO_2$. Such a rapid capacity decrease in samples prepared at 600 and 700°C is due to the uniform formation of the solid solution, *o*-$LiMn_{1-x}Al_xO_2$, across the particle. A higher capacity in the coated $LiMnO_2$ prepared at lower temperatures may be due to the formation of a thin solid solution at

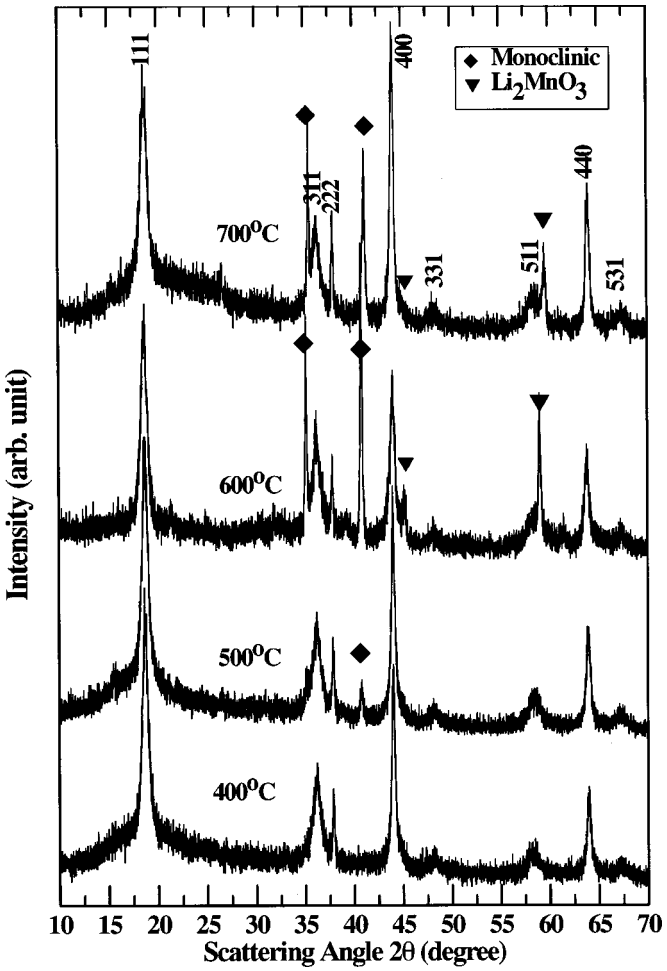

Figure 5. XRD patterns of cycled *o*-$LiMnO_2$ electrodes. The cells were held at 2 V of constant voltage mode for 20 h.

the particle surface. In addition, capacity retention of the coated electrodes appears to deteriorate with increasing heat-treatment temperatures, showing 2, 6, 30, and 33% losses of discharge capacities after 50 cycles (Fig. 4b). This again shows that the capacity retention is effective with a thin coating of $LiMn_{1-x}Al_xO_2$ on the $LiMnO_2$ powders. However, capacity retention of the coated sample prepared at 700°C, in which $LiMn_{1-x}Al_xO_2$ was formed uniformly across the particle, is much worse than that of the homogeneous *o*-$LiAl_{0.05}Mn_{0.95}O_2$, which shows only a 3% capacity loss after 50 cycles.[4] Such a difference may be due to the different C rates used. Chiang *et al.*[4] used charge and discharge current rates of 150 and 75 mA/g, which are five and two times, respectively, faster than this study (36 mA/g for charge and discharge). Slower C rate tests at an elevated temperature caused higher capacity fading in the $LiMn_2O_4$ spinels.[21] At room-temperature cycling of the uncoated and coated electrodes, no capacity fading was observed after 50 cycles.

Structural studies were conducted on cycled electrodes discharged to 2 V after 50 cycles, as shown in Fig. 5. The XRD patterns clearly show that the major crystalline phases exhibit an overall cubic symmetry, irrelevant of the Al concentration. Note that the amount of monoclinic and Li_2MnO_3 phases increased with higher heat-treatment temperatures. Hence, coated electrodes prepared at 600 and 700°C consist of a majority of cubic, with a minor concentration of Li_2MnO_3 and monoclinic phases. On the other hand, coated $LiMnO_2$ specimens prepared at 400°C have only cubic phase after 50 cycles. The formation of the monoclinic phase gets reduced as the Al atoms remain at the particle surface, indicating that

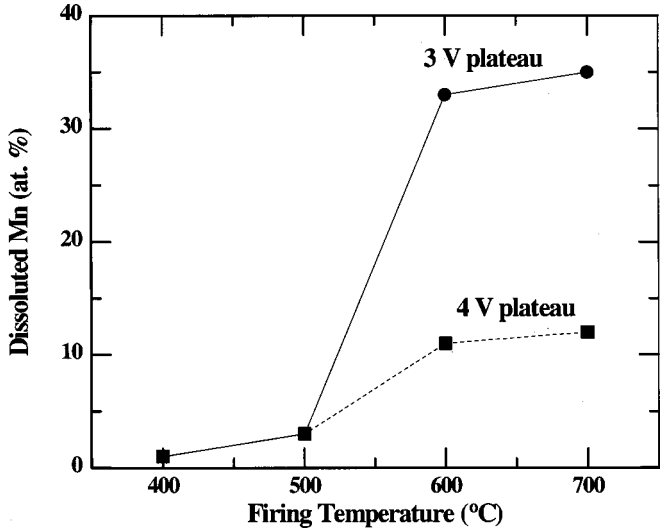

Figure 6. Plots of Mn dissolution (atom %) of coated electrodes prepared at 400, 500, 600, and 700°C. The electrodes were floated at 3.95 and 2.5 V for 15 days at 55°C.

~1 μm thin coating of $LiMn_{1-x}Al_xO_2$ at the surface effectively suppresses the formation of the cycling-induced monoclinic phase. The formation of the Li_2MnO_3 phase was reported to be caused mainly by Mn dissolution from the $Li_2Mn_2O_4$ tetragonal spinel (space group $I4_1/amd$).[17] In order to study Mn dissolution from the bare and coated electrodes, half-cells were floated at the end of the 4 and 3 V plateaus (3.95 and 2.5 V, respectively) at constant-voltage modes for 20 h. (During six cycles, the cells were cycled at charge and discharge rates of 0.01 C.) The electrodes were then dissembled from the half-cells in the glove box, and kept in tightly sealed vials containing constant amounts of the electrolytes at 55°C for 15 days. The 4 and 3 V plateaus correspond to $0 < x \leq 1$ and $1 < x \leq 2$, respectively, in $Li_xMn_2O_4$, where the Li atoms insert at the 8a tetrahedral sites and the 16c octahedral sites, respectively. Inductively coupled plasma (ICP) mass spectroscopy of the electrodes shows a distinct difference upon heat-treatment temperatures, as shown in Fig. 6. Mn dissolution in the electrodes floated at 2.5 V rapidly increases, compared to those floated at 3.95 V.

Furthermore, Mn dissolution proceeds much faster in the cathodes prepared at 600 and 700°C, than those prepared at 400 and 500°C. These results indicate that not only is $Li_2Mn_2O_4$ more structurally unstable than $LiMn_2O_4$ in an acidic electrolyte, but also the uniform (deep) formation of a solid solution across the particle is not effective in preventing Mn dissolution from the particle.

This argument is also supported by examining the capacities on the two voltage plateaus with cycling. While the coated samples prepared at 400°C show almost no capacity decreases at both the 4 and 3 V plateaus, those prepared at 700°C show a significant 3 V capacity decrease, thus showing 7 mAh/g after 50 cycles (Fig. 7a and b). However, the 4 V capacity loss was 34% (from 45 to 30 mAh/g), indicating that the $LiMn_2O_4$ phase was transformed to defect-type spinels. The formation of these spinels cannot be identified by XRD because the diffraction peaks of those phases are superimposed on each other. Nonetheless, the degree of peak broadening indicates the formation of such defective spinels (Fig. 5). The results show that tetragonal $Li_2Mn_2O_4$ spinel is converted to rock salt Li_2MnO_3 during cycling. However, this contradicts the observation that *o*-$LiMnO_2$ appears to have no capacity fading over the 4 and 3 V plateaus during room-temperature cycling, while the XRD patterns of the cycled electrode clearly show increased peak broadening.[5] This can be attributed to the small crystallite size and increased lattice strain, but not to Mn dissolution.

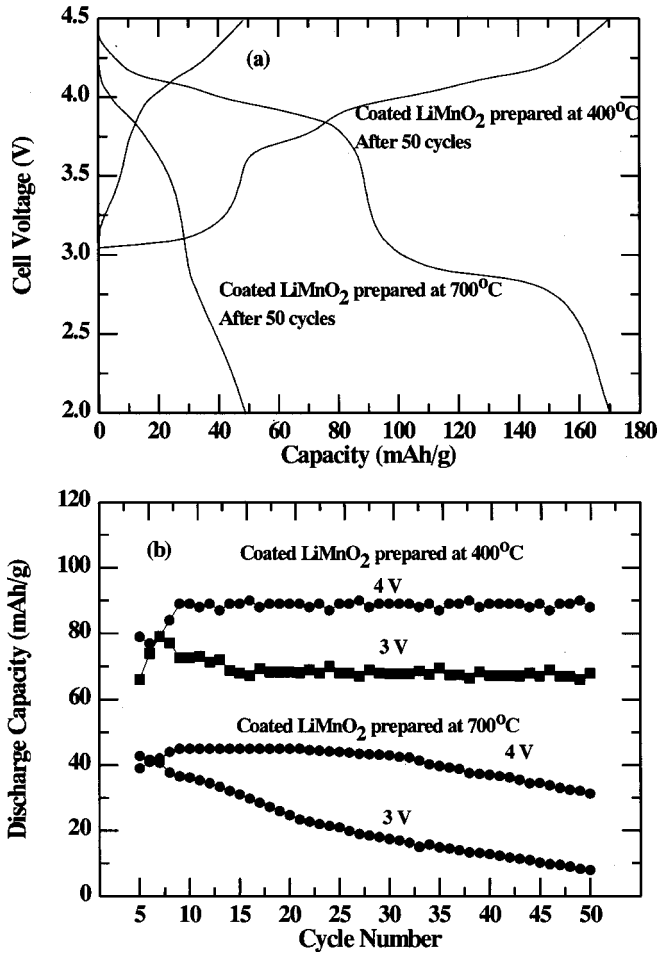

Figure 7. Plots of (a) cell voltage *vs.* capacity in coated $LiMnO_2$ prepared at 400 and 700°C after 50 cycles, and (b) evolution of 4 and 3 V discharge capacities *vs.* cycle number for coated $LiMnO_2$ prepared at 400 and 700°C tested in coin-type half-cells between 4.5 and 2 V. Capacities of 4 and 3 V were calculated in the voltage ranges of 3.5 to 4.5 V and 2.4 and 3.5 V, respectively.

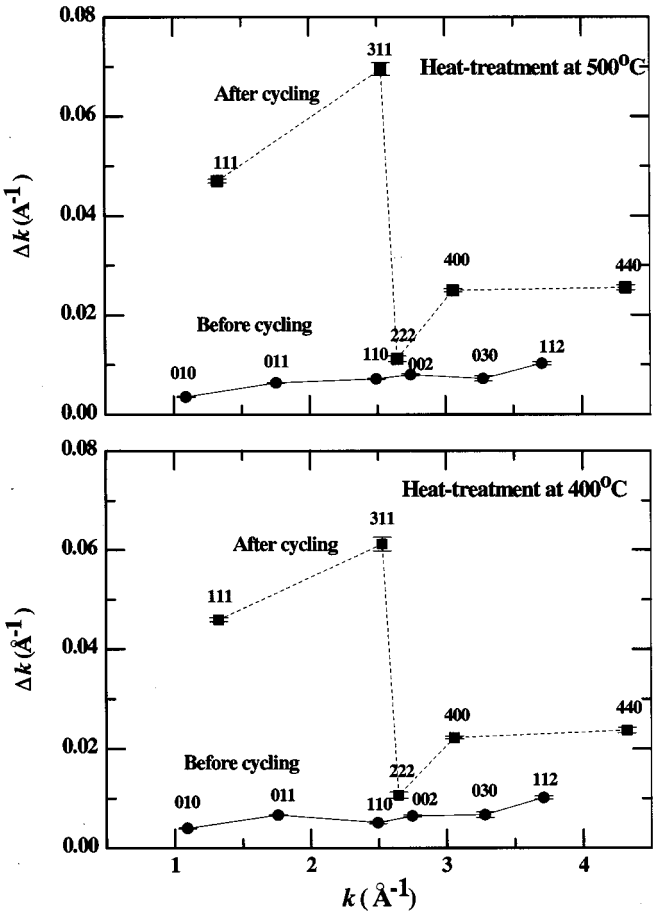

Figure 8. Plots of Δk *vs.* k in the coated $LiMnO_2$ electrodes before and after cycling.

On the other hand, peak broadening in the coated samples prepared at 400 and 500°C can be attributed to other reasons, since both ICP analysis and the capacity-evolution plot at the 4 and 3 V plateaus indicate that Mn dissolution from the $LiMn_2O_4$ and Li_2MnO_3 is not likely to occur. Instead, such broadening may be associated with the small crystallite size and/or lattice strain. To confirm this, XRD peak widths Δk (FWHM) were fit for each peak with the scattering vector $k = (4\pi/\lambda)\sin\theta$ (Fig. 8). A resolution function ($\Delta k_{resol} = 0.0046$ Å^{-1}) was subtracted after fitting each diffraction peak to consider the instrumental broadening effect in diffraction. As shown in Fig. 8, Δk has increased from $\Delta k = 0.0065 \pm 0.0021$ Å^{-1} (averaged from (010) up to (112) peaks) before cycling to $\Delta k = 0.0328 \pm 0.0204$ Å^{-1} (averaged from (111) up to (440) peaks) after cycling in electrodes at 400°C, indicating that the small crystallite size (on the order of a few hundred angstroms) and/or lattice strains were developed during cycling. Similar trends are observed in the coated sample prepared at 500°C. Further studies are currently under way to separately identify the broadening mechanisms of the low-index peaks, (111) and (311), and high-index peaks, (222), (400), and (440).

Conclusions

Al_2O_3-coated $LiMnO_2$, prepared at 400°C for 10 h, exhibited both the least capacity loss and Mn dissolution compared to those prepared at 500, 600, and 700°C. A higher concentration of Al atoms at the surface than in the bulk apparently stabilizes the cubic $LiMn_2O_4$ and tetragonal $Li_2Mn_2O_4$ lattices during cycling. However, when Al atoms diffused more deeply (uniformly) into the particle ($LiMn_{1-x}Al_xO_2$), capacity retention deteriorates. The increased degree of peak broadening after cycling in the coated cathodes prepared at lower temperatures was associated with the formation of nanosize crystallites and/or lattice strains, while peak broadening in those cathodes prepared at higher temperatures originated from Mn dissolution.

Acknowledgment

This work is supported by Samsung SDI Co. and Korea Science & Engineering Foundation, through University-Industry Cooperative Program.

Seoul National University assisted in meeting the publication costs of this article.

References

1. W. D. Johnston and R. R. Heikes, *J. Am. Chem. Soc.*, **78**, 3255 (1956).
2. R. J. Gummow and M. M. Thackeray, *J. Electrochem. Soc.*, **141**, 1178 (1994).
3. J. N. Reimers, E. W. Fuller, E. Rossen, and J. R. Dahn, *J. Electrochem. Soc.*, **140**, 3396 (1993).
4. Y. Chiang, D. R. Sadoway, Y. Jang, B. Huang, and H. Wang, *Electrochem. Solid-State Lett.*, **2**, 107 (1999).
5. Y. Jang, B. Huang, H. Wang, D. Sadoway, and Y. Chiang, *J. Electrochem. Soc.*, **146**, 3217 (1999).
6. J. B. Goodenough, M. M. Thackeray, W. I. F. David, and P. G. Bruce, *Rev. Chim. Miner.*, **21**, 435 (1981).
7. M. M. Thackeray, P. J. Johnson, L. A. de Picciotto, P. G. Bruce, and J. B. Goodenough, *Mater. Res. Bull.*, **19**, 179 (1984).

8. M. Thackeray, W. I. F. David, P. G. Bruce, and J. B. Goodenough, *Mater. Res. Bull.*, **18**, 461 (1983).
9. H. Wang, Y. Jang, and Y. Chiang, *Electrochem. Solid-State Lett.*, **2**, 490 (1999).
10. Y. Xia, Y. Zhou, and M. Yoshio, *J. Electrochem. Soc.*, **144**, 2593 (1997).
11. D. H. Jang and S. M. Oh, *J. Electrochem. Soc.*, **144**, 3342 (1997).
12. A. D. Robertson, S H. Lu, and W. F. Howard, Jr., *J. Electrochem. Soc.*, **144**, 3505 (1997).
13. A. Blyr, C. Sigala, G. Amatucci, D. Guyomard, Y. Chabre, and J. M. Tarascon, *J. Electrochem. Soc.*, **145**, 194 (1998).
14. J. Cho, *Solid State Ionics*, **138**, 267 (2001).
15. D. Aurbach and Y. Gofer, *J. Electrochem. Soc.*, **138**, 3529 (1991).
16. R. J. Gummow and M. M. Thackeray, *J. Electrochem. Soc.*, **141**, 1178 (1994).
17. J. Cho and M. M. Thackeray, *J. Electrochem. Soc.*, **146**, 3577 (1999).
18. J. Cho, G. Kim, H. Lim, C. Kim, and S. I. Yoo, *Electrochem. Solid-State Lett.*, **2**, 607 (1999).
19. J. Cho, Y. J. Kim, and B. Park, *Chem. Mater.*, **12**, 3788 (2000); J. Cho, Y. J. Kim, T.-J. Kim, and B. Park, *Angew. Chem. Int. Ed.*, **40**, 3367 (2001).
20. L. Croguennec, P. Deniard, R. Brec, and A. Lecerf, *J. Mater. Chem.*, **7**, 511 (1997).
21. J. C. Rousche, MMM, Belgium, Personal communication.